Chemico-Biological Interactions xxx (2009) xxx–xxx

Contents lists available at ScienceDirect

Chemico-Biological Interactions

journal homepage: www.elsevier.com/locate/chembioint

Inflammation-associated gene transcription and expression in mouse lungs induced by low molecular weight compounds from fungi from the built environment

J.D. Miller[a], M. Sun[b], A. Gilyan[b], J. Roy[b], T.G. Rand[b,*]

[a] Department of Chemistry, Carleton University, Ottawa, Ontario, Canada K1S 5B6
[b] Department of Biology, Saint Mary's University, 923 Robie St., Halifax, Nova Scotia, Canada B3H 3C3

ARTICLE INFO

Article history:
Received 22 August 2009
Received in revised form
29 September 2009
Accepted 29 September 2009
Available online xxx

Keywords:
Fungi
Atranones
Brevianamide
Cladosporin
Mycophenolic acid
Neoechinulins
Sterigmatocystin
TMC-120A
Mouse lungs
Inflammation-associated genes
(RT)-PCR arrays

ABSTRACT

Few metabolites from fungi found indoors have been tested for inflammatory mediators endpoints in primary cultures of alveolar macrophages or *in vivo*. In this study, mice were intratracheally instilled with a single dose comprising 4×10^{-5} mole toxin/kg lung wt dose of either atranone C, brevianamide, cladosporin, mycophenolic acid, neoechinulin A & B, sterigmatocystin or TMC-120A. These toxins are from fungi common on damp building materials. The dose used was comparable to the estimated doses of possible human exposure. Hematoxylin and eosin (H&E) histology and Alcian Blue/Periodic Acid Schiff (AB/PAS) histochemistry were used to evaluate lungs for time course (4 h and 12 h post-exposure (PE)) inflammatory and toxic changes. Reverse-transcription (RT)-PCR based arrays were also employed to evaluate time course inflammation-associated gene transcription in lung tissues of the different toxins. Immunohistochemistry (IHC) was used to probe MIP-2 and Tnf-α protein expression in treatment lungs to determine whether responses correspond with gene transcription data. Both histology and histochemistry revealed that toxin exposed lungs at 12 h PE showed evidence of inflammation. H&E revealed that bronchioli were lined with irregularly thickened and sometimes sloughing epithelium and bronchiolar spaces supported infiltration of leukocytes, cellular and mucus-like debris while alveolar spaces supported swollen macrophages and modest amorphous debris accumulations. All toxin-instilled lungs exhibited copious mucus production and alveolar macrophages with red stained cytoplasm on bronchiolar surfaces, especially at 12 h PE. Array analysis of 83 inflammation-associated genes extracted from lung tissue demonstrated a number of patterns, compared to controls. 82 genes assayed at 4 h PE and 75 genes at 12 h PE were significantly altered ($p \leq 0.05$; ≥1.5-fold or ≤−1.5-fold change) in the different treatment animal groups. Expression of transcriptionally regulated genes was confirmed using immunohistochemistry that demonstrated MIP-2 and Tnf-α staining in respiratory bronchiolar epithelia, alveolar macrophages and alveolar type II cells. The transcriptional regulation in these genes in the treatment groups suggests that they may serve central roles in the immunomodulation of toxin-induced pro-inflammatory lung responses. Hierarchical cluster analysis revealed significant patterns of gene transcription linking the response of the toxins at equimolar doses in three groups: (1) brevianamide, mycophenolic acid and neoechinulin B, (2) neoechinulin A and sterigmatocystin, and (3) cladosporin, atranone C and TMC-120. The results further confirm the inflammatory nature of metabolites/toxins from such fungi can contribute to the development of non-allergenic respiratory health effects.

1. Introduction

Inhaled fungal spores and mycelial fragments contain allergens, fungal glucan, and low molecular weight metabolites. Although the largest of these particles do not reach the lungs in high efficiency nor penetrate deeply, the smallest do [1]. Altered lung physiology might result from low dose exposures to all these components [2]. Effects might be additive and include damage to the macrophage system thus interfering with the particle clearance system of the lung and other processes mediated by lung and other cells extending beyond the lung [3–5].

Several studies have demonstrated the inflammatory potential of fungal spores using rodent models of lung disease. We had previously shown that acute lung inflammation results from low dose exposure to the spores of the atranone- and trichothecene-producing strains of *S. chartarum sensu lato* and hypothesized that

* Corresponding author. Tel.: +1 902 475 1456; fax: +1 902 475 1982.
E-mail address: thomas.rand@smu.ca (T.G. Rand).

0009-2797/$ – see front matter © 2009 Published by Elsevier Ireland Ltd.
doi:10.1016/j.cbi.2009.09.023

Table 1
Toxins used, their molecular formulae and weights and doses intratracheally instilled into mouse lungs.

Toxin	Molecular formula	Molecular weight	μg/kg lung wt[a]	mole/kg lung wt
Atranone C	$C_{24}H_{34}O_4$	416.22	177.7 ± 56.3	4×10^{-5}
Brevianamide A	$C_{21}H_{23}N_3O_3$	365.43	156.0 ± 49.2	4×10^{-5}
Cladosporin	$C_{16}H_{20}O_5$	292.13	124.7 ± 39.5	4×10^{-5}
Mycophenolic acid	$C_{17}H_{20}O_6$	320.24	136.7 ± 43.3	4×10^{-5}
Neoechinulin A	$C_{19}H_{21}N_3O_2$	323.16	140.0 ± 43.7	4×10^{-5}
Neoechinulin B	$C_{19}H_{19}N_3O_2$	321.15	137.1 ± 43.4	4×10^{-5}
Sterigmatocystin	$C_{18}H_{12}O_6$	324.28	138.4 ± 43.8	4×10^{-5}
TMC-120A	$C_{15}H_{15}NO_2$	241.11	102.9 ± 32.6	4×10^{-5}

[a] Mean lung wt = 0.25 ± 0.026 g (n = 25); mean BW = 24.413 ± 2.029 g (n = 25).

this response reflected exposure to the low molecular weight compounds sequestered in the spores [6]. This prompted studies of a number of pure compounds arising from two fungi common in the built environment [7] using an *in vivo* mouse model [8,9] which suggested that these were potently inflammatory and apparently immunomodulatory. More recently, we found that the pure (1 → 3)-β-D glucan, curdlan, was potently inflammatory, inducing significant inflammation-associated gene modulation at dose as low as 4 ng curdlan/kg lung wt in our mouse model of lung disease [1]. The strongest inflammatory response was in the intratracheally instilled lungs exposed to 4 μg curdlan/kg lung wt, with the number of modulated genes falling off sharply at the lower doses (0.4 μg to 4 ng curdlan/kg lung wt).

The fungi common on moldy building materials comprise species adapted to the nutrients available and further affected by moisture content. The toxins in this study come from common damp building fungi [7] associated with (1) high water activity: *Stachybotrys chartarum*, *S. chlorohalonata* (atranone C), (2) intermediate water activities: *Penicillium brevicompactum* (brevianamide, mycophenolic acid), *Aspergillus versicolor* (sterigmatocystin) and *A. insuetus*/*A. calidoustus* = *A. ustus sensu lato* (TMC-120A) and (3) low water activity building materials: *Eurotium amstelodami*, *E. herbariorum* and *E. rubrum* (neoechinulin A & B) and cladosporin from *E. herbariorum*.

There are few data on the occurrence of these eight compounds on damp building materials or on their toxicity [10–35] and only three have been demonstrated to potentiate pulmonary inflammation [8,9]. Intratracheal exposure to atranone C was previously studied in Swiss Webster mouse lungs. Macrophage and neutrophil concentrations in BAL were reduced at ∼0.1 μM on a fresh lung weight basis. Estimated on the same basis, *MIP-2*, *TNFα* and *IL-6* at 3 h were increased at 0.05, 0.5, and 0.02 μM, respectively [9]. Intratracheal exposure to brevianamide and mycophenolic acid was also previously studied in Swiss Webster mouse lungs. Macrophage and neutrophil concentrations in BAL were reduced at ∼1.5 μM on a fresh lung weight basis and estimated on the same basis, *MIP-2* at 3 h was increased at 1.5 μM in brevianimide exposed animals (calculated from [8]). No effects were seen on macrophage and neutrophil concentrations in BAL nor changes in *MIP-2*, *TNFα* or *IL-6* at 3 h observed using mycophenolic under the conditions tested [8]. Because the inflammatory potential of these compounds from fungi that grow on damp building materials is only poorly understood and because molecular mechanisms underscoring inflammatory lung responses is not understood for any, we decided that further work was needed to evaluate their role on the acute inflammatory response in a rodent model of lung disease.

In this study, we compare inflammatory lung responses to 8 metabolites/toxins from fungi that are commonly recovered from damp building materials (brevianamide A, cladosporin, mycophenolic acid, neoechinulin A & B, sterigmatocystin, TMC-120A (hereafter TMC-120) and atranone C). Using our mouse model of lung disease, the objectives of this study were to evaluate mouse lungs intratracheally exposed to a single dose of 4×10^{-5} mole toxin/kg lung wt for histological and histochemical (for mucus production) responses at 4 h and 12 h post-exposure (PE). They were also to evaluate time course (4 h and 12 h PE) profiles associated with pro-inflammatory gene transcriptional responses using mouse inflammatory gene and receptor arrays and reverse-transcription (RT)-PCR to determine whether responses are linked to inflammatory cell recruitment and activation, and *MIP-2* and *Tnf-α* immunohistochemistry. The immunohistochemical experiments were performed to determine whether responses correspond with gene transcription data, especially as concentrations of both of these cytokines have been shown to be significantly elevated in bronchioalveolar lavage fluid (BALF). The mice were intratracheally exposed to doses of 4×10^{-5} mole toxin/kg lung wt of the above metabolites, respectively. The equimolar dose used was comparable to the lowest effect level for the few of these compounds tested in primary and immortalized cells [10,13,20,28,33,35].

2. Materials and methods

2.1. Toxin preparations

Atranone C, brevianamide A and mycophenolic acid were isolated and the purity (>98%) documented as previously described [8,9]. Cladosporin, neoechinulin A & B, and TMC-120 were isolated and the purity documented as described in [36]. Sterigmatocytin from *A. versicolor* was purchased from Sigma–Aldrich, Canada (S3255). Fungi do not produce endotoxin, isolation conditions preclude its presence, and solutions were prepared with endotoxin-free water and glassware. For the animal studies, toxins were dissolved in 10% ethanol, diluted in pyrogen-free PBS to 10^{-6} M working solution and prepared fresh before the *in vivo* experiments. They were then diluted to working solutions and all toxins were administered intratracheally as a single dose.

2.1.1. Animals

All mice used in the experiments were housed according to the standards of the Canadian Council for Animal Care [37] and with approval from the Dalhousie University Animal Care Committee. The mice were given food and water *ad libitum* and acclimatized for 1-week prior to use.

2.1.2. In vivo experiments

A total of 90 random-bred, pathogen-free Carworth Farms white (CFW) Swiss Webster 21- to 28-day-old male mice (23 ± 1.2 g) were divided into 9 treatment groups (control, atranone C, brevianamide, cladosporin, mycophenolic acid, neoechinulin A & B, sterigmatocystin and TMC-120). The control and treatment animals were separated into two groups of five mice each to test for time-dependent effects. All treatment mice were exposed to 4×10^{-5} mole toxin/kg lung wt by intratracheal instillation. Because compounds were of differing molecular weights were tested (241–416 MW), equimolar doses were used ranging from ca. 100 to 177 μg/mg lung weight (Table 1).

Please cite this article in press as: J.D. Miller, et al., Inflammation-associated gene transcription and expression in mouse lungs induced by low molecular weight compounds from fungi from the built environment, Chem. Biol. Interact. (2009), doi:10.1016/j.cbi.2009.09.023

Time course effects were studied at 4 h and 12 h PE. The two groups of five control animals were intratracheally instilled with carrier saline only.

Before instillation, mice were lightly anaesthetized with an intraperitoneal injection (IP) of 0.3 ml of an anaesthetic mixture consisting of: 30% ketamine (Ketaleen®; 100 mg/ml), 5.2% xylazine (Rompun®; 100 mg/ml), and 64.8% physiological saline. Once anaesthetized, each mouse was placed on an intratracheal instillation board 20° from the vertical as described in [8,9] and instilled with 50 μl of toxin solution, as described above. Control animals were instilled with 50 μl of carrier saline only. Mice were left in the upright position on the instillation board for approximately 2 min before being placed back in their cages on a warm pad to recover. During recovery, mice were monitored for signs of sickness or distress as outlined in CCAC guidelines [37].

Groups of five mice for each treatment were killed at 4 h and 12 h post-exposure (PE). Mice were euthanized using with a 0.3 ml IP injection of Euthanol® (sodium pentobarbital (54.7 mg/ml)). The mice were immediately exsanguinated by cutting the abdominal artery and the lungs were removed. The right lung was immersed immediately in 5 ml of ice-cold RNAlater® then teased with forceps to remove the major respiratory tree components (i.e. trachea, bronchus and large bronchioli) as per [1]. The tissue was suspended in 1 ml RNAlater® and stored at −20 °C for later study. The left lung was excised and immediately fixed in fresh 4% paraformaldehyde in 0.1 M phosphate-buffered saline (PBS) pH 7.3, prepared using diethylpyrocarbonate water (DEPC-water), for 6 h, for H&E staining, muco-substance histochemistry, and *MIP-2* and *Tnf-α* immunohistochemistry (IHC).

2.1.3. Histology

For routine processing, fixed lung tissues from 4 animals/group were rinsed in tap water, dehydrated through an ascending ethanol series, cleared in xylene, embedded in paraffin and sectioned until all lung lobes were represented in the sectioning plane. Six-μm-thick sections were then cut and mounted onto microscope slides for hematoxylin and eosin (H&E) staining.

2.1.4. Histochemistry

Because H&E staining revealed the presence of lightly stained eosinophilic, mucus-like accumulations in the lungs, especially in the bronchiolar airways of some treatment animals, the Alcian Blue (pH 2.5)/Periodic Acid Schiff (PAS) test for acid and 1,2-linked muco-polysaccharides in respiratory airways and alveolar spaces. All histochemical experiments were done using the same 4% paraformaldehyde-fixed lung tissue blocks employed for histology. All tissue sections were stained using techniques described in [38,39] as follows: Harris' Hematoxylin and alcoholic eosin (H&E); and Alcian Blue/PAS (AB/PAS) method for muco-substances, pH 2.5.

2.1.5. RNA extraction and reverse-transcription real-time PCR

Total RNA isolation was performed using Trizol® reagent (Gibco BRL) according to the manufacturer's specifications. Briefly, right lung tissues were homogenized in 1 ml of Trizol® reagent using a CAT ×120 electric homogenizer (Rose Scientific Ltd, Edmonton Alta.). After addition of chloroform and centrifugation at 4 °C the aqueous layer was recovered and RNA was precipitated with isopropanol. The precipitated RNA solution was again centrifuged at 4 °C to pellet the RNA. The RNA pellet was washed with 75% ETOH and re-suspended in RNAse free water (Sigma–Aldrich). The concentration of RNA in samples was determined using a NanoDrop® ND-1000. RNA integrity and purity was assessed using an Agilent 2100 Bioanalyzer. Samples with 260/280 nm ratio of ≥2.0 were used for array analysis.

2.1.6. Reverse-transcription real-time PCR and array analysis

Reverse-transcription PCR reactions were carried out using a reaction ready first strand cDNA synthesis kit (SuperArray, Bioscience Corp.) according to manufacturer's instructions. The reverse-transcription and real-time PCR reactions were carried out using 96-well PCR arrays designed for the evaluation of mouse inflammatory genes and receptors (# PAMM-022 SuperArray Bioscience Corp®) and using an ABI Prism 7000 Sequence Detection System (Applied Biosystems). Relative gene expression was determined according to the comparative C_t method, with the β-actin (Actb) housekeeping gene and negative control references for DNA contamination set as the calibrators. Fold change equals $2^{\Delta\Delta C_t}$, where the C_t is the threshold cycle, ΔC_t is the difference between the C_t values of the target gene and the internal control gene, $\Delta\Delta C_t$ represents the difference between the ΔC_t value for the control and treated lung tissues.

2.2. Statistical analysis

Genes and treatment groups were clustered using the SuperArray web-based hierarchical clustering software package for the PCR Array System (http://www.sabiosciences.com/pcrarraydataanalysis.php). A Shapiro–Wilks test for normality was performed to verify if the samples were normally distributed. A two-tailed unpaired *t*-test ($p \leq 0.05$) was then performed to determine if the treatments showed significant inflammatory gene expression in comparison with the controls. All data are shown as their mean fold change values. One-way ANOVA and Tukey's pair-wise analyses were also carried out using SYSTAT version 11.0. Gene transcription results were considered significant if they had ≥1.5-fold or ≤−1.5-fold change at $p \leq 0.05$ probability level.

2.2.1. Immunohistochemistry (IHC)

Induction of *MIP-2 and Tnf-α* expression: To confirm gene array data that cytokine gene transcription was being translated to cytokine protein expression in treatment lungs, immunohistochemistry was used to detect two cytokines, *MIP-2* and *Tnf-α* expression in the same 4% paraformaldehyde-fixed lung tissues employed for histology. IHC procedures employing a Heat-Induced Epitope Retrieval (HIER) protocol have been described previously [1], with the following modest exception. After blocking, test slides were exposed to polyclonal Goat Anti-MIP-2-BIOT Fab-fragments 1:75 (R&D Systems) in 0.01 M PBS (pH 7.6), or polyclonal Goat Anti-*Tnf-α*-BIOT Fab-fragments 1:75 (R&D Systems) in 0.01 M PBS (pH 7.6), solution while negative control slides were exposed only to PBS. Positive control tissue was mouse skin which exhibits positive staining results with both MIP-2 and *Tnf-α* [1]. Test and control slides were incubated in a humid chamber at 37 °C for 2 h. After incubation, slides were rinsed 2× in PBS (pH 7.6), 4 min each followed by rinsing 2× in Tris–HCl (pH 7.6) at 4 min each. After rinsing, slides were covered with 70 μl of a 1:250 Anti-Biotin-Alkaline Phosphatase, Fab-fragments (AB Roche Molecular Biochemicals) in 0.05 M Tris–HCL (pH 7.8) and incubated in a humid chamber at 37 °C for 45 min. After incubation, slides were rinsed 3× in Tris–HCl (pH 7.6), 4 min each and then in Buffer II (=100 mL Tris-Base (pH 9.5); 0.580 g NaCl; 1.015 g $MgCl_2$) solution at room temperature for 10 min. After color reaction and color development, slides were rinsed 3× in Tris–HCl (pH 8.0) buffer solution, 4 min each, dehydrated in an ascending ETOH series and mounted using Hydromatrix®, as described by [1].

All imaging was with a Leica DMRE microscope with Simple PCI image capture system (Compix, C-Imaging Systems, Cranberry Township, PA, USA).

Please cite this article in press as: J.D. Miller, et al., Inflammation-associated gene transcription and expression in mouse lungs induced by low molecular weight compounds from fungi from the built environment, Chem. Biol. Interact. (2009), doi:10.1016/j.cbi.2009.09.023

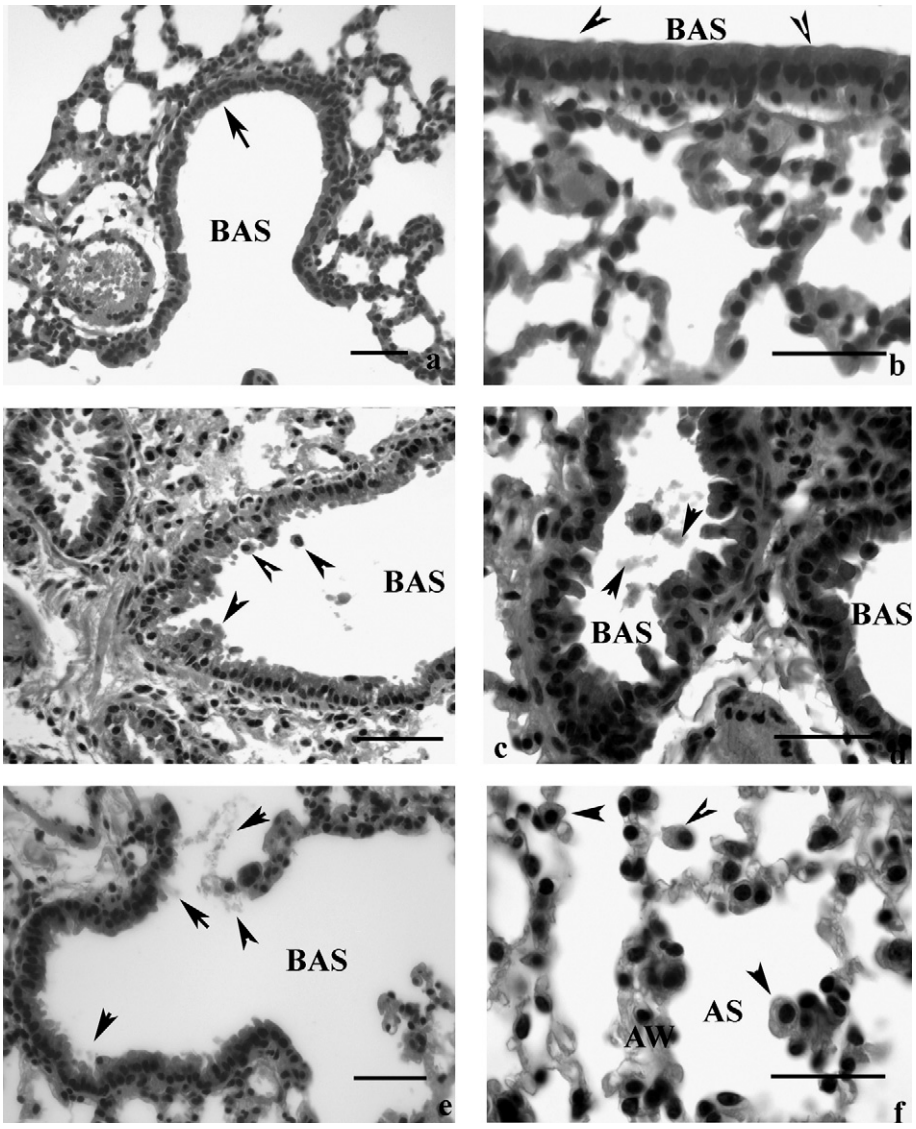

Fig. 1. H&E staining of carrier control (a and b) and toxin-instilled lung tissues at 12 h PE (c–f). Note that alveolar and alveolar and bronchiolar spaces lack evidence of leukocyte infiltration and the generally uniform appearance of bronchiolar cuboidal epithelium with smooth or slightly raised apical surfaces that lacked apparent mucus accumulation (arrows) in carrier control lungs (a and b). Bronchiolar and alveolar spaces and epithelium of all toxin treated lungs showed signs of inflammation. Mycophenolic acid (c) and neoechinulin B (d) treated lungs that show that bronchioli were lined with irregularly thickened and sometimes sloughing epithelium; bronchiolar spaces of mycophenolic acid (c), neoechinulin B (d) and sterigmatocystin (e) treatment lungs also supported infiltration of leukocytes, and cellular and/or mucus-like debris. In mycophenolic acid, neoechinulin A & B and sterigmatocystin (f) treatment lungs, alveolar walls appeared edematous. Alveolar surfaces and adjacent spaces of all treatment lungs also supported macrophages (f). AW = alveolar walls; AS = alveolar space; BAS = bronchiolar space. Bar scales = 20 μm. All treatment lungs were instilled with 4×10^{-5} mole toxin/kg/lung wt.

3. Results

None of the control or treatment animals used in the experiments showed signs of illness or respiratory distress due to instillation procedures.

3.1. Histology

Hematoxylin and eosin (H&E) staining revealed that alveolar spaces of vehicle control lungs lacked erythrocytes, leukocyte infiltration and cellular debris (Fig. 1a and b) at both 4 h and 12 h PE. Terminal bronchioli and secondary bronchioles were lined with uniformly thick, cuboidal epithelium with smooth or slightly raised apical surfaces (Fig. 1a and b) and lacked a conspicuous mucus film (Fig. 1b). It also revealed that treatment lungs were similar to those of carrier controls at 4 h PE. However, at 12 h PE, bronchiolar and alveolar spaces and epithelium of all toxin treated lungs showed light signs of inflammation, and especially in mycophenolic acid (Fig. 1c), neoechinulin B (Fig. 1d) and sterigmatocystin (Fig. 1e and f) treatments. Bronchioli were lined with irregularly thickened and sometimes sloughing epithelium and bronchiolar spaces supported infiltration of leukocytes (Fig. 1c and d), and cellular and mucus-like debris (Fig. 1c–e). In mycophenolic acid (Fig. 1c), neoechinulin A & B (Fig. 1d) and sterigmatocystin (Fig. 1f) treatment lungs, alveolar walls appeared edematous. All treatment lungs also supported swollen macrophages in alveolar spaces and loosely associated with alveolar wall surfaces (Fig. 1f), and modest amorphous debris accumulations (not shown).

3.2. Histochemistry

Alcian Blue (AB)/Periodic Acid Schiff (PAS) staining revealed that bronchiolar epithelial surfaces and spaces of carrier control lungs lacked erythrocytes, leukocyte infiltrates, cellular debris or mucus film (Fig. 2a). It also revealed that all toxin-instilled lungs especially at 12 h PE exhibited copious mucus production.

Please cite this article in press as: J.D. Miller, et al., Inflammation-associated gene transcription and expression in mouse lungs induced by low molecular weight compounds from fungi from the built environment, Chem. Biol. Interact. (2009), doi:10.1016/j.cbi.2009.09.023

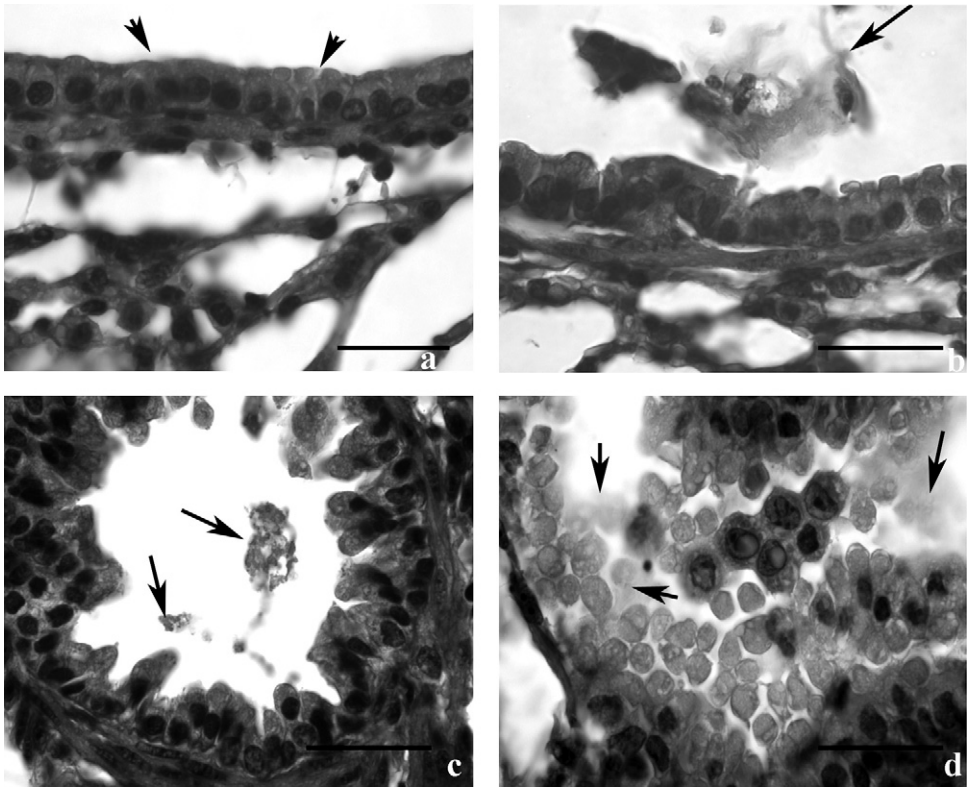

Fig. 2. AB/PAS stained carrier control (a) and toxin-instilled (b–d) at 12 h PE. Note carrier bronchiolar epithelium of carrier control lung lacks an apparent mucus film (arrows) (a). Apical bronchiolar epithelial surfaces of atranone C (b), neoechinulin B (c) and cladosporin (d), and bronchiolar spaces of neoechinulin B (c) instilled lungs showing that they supported copious positively stained muco-substances (arrows), and alveolar macrophages with positively stained cytoplasm, especially in neoechinulin A treatments (d). AW = alveolar walls; AS = alveolar space; BAS = bronchiolar space. Bar scales = 20 μm. All treatment lungs were instilled with 4×10^{-5} mole toxin/kg/lung wt.

Mucus was manifest as variable quantities of deep blue (=sialylated mucins), red (=sulfated mucins), or variably purple (=mixture of sialylated/sulfated mucins) stained muco-substances in bronchiolar spaces and on apical bronchiolar epithelial surfaces, especially in atranone C (Fig. 2b) and neoechinulin B (Fig. 2c) treatments (colors not shown). Additionally, bronchiolar spaces also contained variable numbers of alveolar macrophages with red stained cytoplasm, especially in neoechinulin A treatment animals (Fig. 2d).

3.3. Toxin-induced inflammation-associated gene modulation

Tukey's pair-wise comparisons revealed that, compared to controls, 82 of the 83 inflammation-associated genes assayed at 4 h post-exposure (PE) were significantly modulated (up- or down-regulation), while at 12 h PE, 75 genes were significantly transcribed in the different treatment animal groups. However, not all of these regulated genes were transcribed in all treatment animals (Table 2). Heat map profiling (Fig. 3a and b) revealed that compared to controls, the patterns of significant gene expression in treatments at both 4 h and 12 h PE were different. At 4 h PE, there were at least three clusters. One cluster representing all treatments, except neoechinulin B, comprised *Il20*, *Cxcr3*, *Ccl19*, *Cx3cl1*, *Abcf1*, *Il10rb1*, *Mif*, and *Tnfrsf1a*. A second cluster representing all treatments, except atranone C and neoechinulin B, comprised *ILr1*, *Ltb*, *Ccl25*, *Cd40lg*, *Cxcl15*, *Il6st*, *Il2rb*, *Ccr2*, *Il16*, *Ccl8* and *Il3*. The third cluster representing all treatments except neoechinulin B comprised *Scye1*, *Itgb2*, *Spp1*, *Il1f6* and *tollip* (Fig. 3a). At 12 h PE signs of clustering were not as apparent as in the 4 h PE treatments (Fig. 3b).

The highest number of significantly changed gene transcripts (68/83) was in TMC-120 treatment animals at 12 h PE, followed by sterigmatocystin (48 at 4 h), atranone C (44 at 12 h) and neoechinulin A (41 at 4 h) (Table 2). The highest up-regulated fold change (7891) as well as the lowest fold change (−504) compared to controls was in the TMC-120 treatment animals at 12 h PE. With the exceptions of atranone C, cladosporin and TMC-120 the majority of significantly modulated genes were at 4 h PE. The number of genes significantly up-regulated at 4 h PE was highest in brevianamide (34/39), neoechinulin A (30/41) and sterigmatocystin (43/48). With the exception of TMC-120 the highest number of significantly down-regulated gene transcripts was also at 4 h PE, with the highest number in the sterigmatocystin treatment (31/36 genes). Of the 83 inflammation-associated genes assayed, 10 (*Abcf1*, *Bir1*, *Ccl19*, *Ccl20*, *Ccr6*, *Cx3cl1*, *Cxcl5*, *Il6st*, *Scye1*, *Tnfrsf1a*) were significantly transcribed in all treatment groups at one time point at least. Sixteen other gene mRNAs were significantly modulated in all but one of the treatment groups (*Ccl4*, *Ccl7*, *Ccl25*, *Ccr2*, *Ccr9*, *Ccr10*, *Cxcl1*, *Cxcl3*, *Cxcr3*, *Ilr1*, *Il2rb*, *Il5ra*, *Il10rb*, *Ltb*, *Tnf-α*, *Cd40lg*) (Table 2).

Patterns of gene transcription also varied amongst the different treatments (Table 2). For example, in the atranone C and cladosporin treatments, the numbers of genes transcribed in the *Ccr* and *Cxcl* families at 12 h was higher than at 4 h PE. For brevianamide, the *Ccl* and *Ccr* gene transcripts at 4 h were more dominant than at 12 h PE. For mycophenolic acid, neoechinulin A & B, *Ccl* and *Cxcl* families were more dominant at 4 h than at 12 h PE. At 4 h PE, sterigmatocystin treatment resulted in the significant transcription of higher numbers of *Ccl*, *Ccr*, *Cxcl*, *Cxcr* and *Il* genes than at 12 h PE. Moreover, intratracheal exposure to this toxin also resulted in the significant transcription of other inflammation-associated genes, including *Ltb*, *Scye1*, *Tnf-α*, *Tnfrsf1a* and *Cd40lg*, at 4 h PE but not at 12 h PE. For TMC-120, expression of all gene families assayed was highest at 12 h PE (Table 2).

To determine the similarity of the gene responses to each toxin, hierarchical cluster analyses of standardized data were

Please cite this article in press as: J.D. Miller, et al., Inflammation-associated gene transcription and expression in mouse lungs induced by low molecular weight compounds from fungi from the built environment, Chem. Biol. Interact. (2009), doi:10.1016/j.cbi.2009.09.023

Table 2
Significant inflammation-associated gene changes in toxin exposed mouse lungs at 4 h and 12 h PE. Positive numbers are significantly up-regulated gene transcripts; negative numbers are significantly down-regulated transcripts (≤1.5-fold or ≥−1.5-fold change at $p \leq 0.05$ probability level). Blank spaces are non-significantly transcribed genes.

RefSeq	Gene	Gene description	Toxin															
			Atranone C		Brevianimide A		Cladosporin		Mycophenolic Acid		Neoechinulin A		Neoechinulin B		Sterigmatocystin		TMC-120	
			4 h	12 h	4 h	12 h	4 h	12 h	4 h	12 h	4 h	12 h	4 h	12 h	4 h	12 h	4 h	12 h
NM_013854	Abcf1	ATP-binding cassette, sub-family F (GCN20), member 1	4.13	4.57	4.48	3.02	9.11	5.95	11.08	2.74	3.25	2.42		2.56	6.93		9.23	
NM_009744	Bcl6	B-cell leukemia/lymphoma 6												1.72				85.5
NM_007551	Blr1	Burkitt lymphoma receptor 1		6.51	7.86	7.38	10.86	8.36	49.48	6.16	12.71	2.4	2.3		11.93		5.83	3.96
NM_009778	C3	Complement component 3	−3.33								4.33							38.14
NM_009807	Casp1	Caspase 1		1.6						1.52						1.53		
NM_011329	Ccl1	Chemokine (C–C motif) ligand 1													5.09			−6
NM_011330	Ccl11	Small chemokine (C–C motif) ligand 11	3.49	5.17		9.43						2.61	−2.92				−9.91	−15.39
NM_011331	Ccl12	Chemokine (C–C motif) ligand 12		2.05	−4.05	2.73							−4.33					7.26
NM_011332	Ccl17	Chemokine (C–C motif) ligand 17											−5.63					2.98
NM_011888	Ccl19	Chemokine (C–C motif) ligand 19	21.32	7.93	9.43	3.41	26.94	8	23.57	3.03	10.12	2.89	−2.09	6.52	26.11		35.03	326.54
NM_011333	Ccl2	Chemokine (C–C motif) ligand 2	−3.1		−8.41						−11.94		−46.75				−10.14	14.98
NM_016960	Ccl20	Chemokine (C–C motif) ligand 20	−41.29	14.77	−71.32	8.45	−14.4		−6.5	6.22	−14.51	3.57	−358.44	3.28	−8.59		−67.77	25.69
NM_009137	Ccl22	Chemokine (C–C motif) ligand 22							3.41				−3.54	2.37	3.3			2.58
NM_019577	Ccl24	Chemokine (C–C motif) ligand 24			2.45	3.17												−17.12
NM_009138	Ccl25	Chemokine (C–C motif) ligand 25	3.51		5.59		3.7		6.04		4.2	1.94			2.39		2.58	2.78
NM_011337	Ccl3	Chemokine (C–C motif) ligand 3	−5	−3.24				−2.22			−3.78	−3.76	−19.93				−5.27	−1.65
NM_013652	Ccl4	Chemokine (C–C motif) ligand 4	−28.32	2.75	−7.66		−3.82		−6.56		−11.39		−84.28				−11.05	33.55
NM_013653	Ccl5	Chemokine (C–C motif) ligand 5			3.43						4.42	3	−2.02					
NM_009139	Ccl6	Chemokine (C–C motif) ligand 6	−5.1	−5.43					5.09	−2.17			1.71					30.88
NM_013654	Ccl7	Chemokine (C–C motif) ligand 7	−3.61		−3.92		−4.45		−6.26		−5.97		−15.56				−8.24	
NM_021443	Ccl8	Chemokine (C–C motif) ligand 8		11.5	3.82	4.48						1.66	2		5.52	3.72		
NM_011338	Ccl9	Chemokine (C–C motif) ligand 9											−7.96					115.69
NM_009912	Ccr1	Chemokine (C–C motif) receptor 1					3.05				2.73		−4.01		4.9			
NM_009915	Ccr2	Chemokine (C–C motif) receptor 2		2.63	10.57	4.74	7.37		24.09	2.96	12.04				5.84			15.37
NM_009914	Ccr3	Chemokine (C–C motif) receptor 3	−2.86	3.04		2.9		3.25	4.08	4.5			−8.72					121.59
NM_009916	Ccr4	Chemokine (C–C motif) receptor 4	3.21	5.31	4.26		7.75	2.44							11.2			−309.76
NM_009917	Ccr5	Chemokine (C–C motif) receptor 5	−4.04	2.18									−5.51				−2.56	24.26
NM_009835	Ccr6	Chemokine (C–C motif) receptor 6	52.7	11.64	11.98	6.24	44	20.52		11.85	10.06	3.36		3.88	40.14	2.3	44.3	
NM_007719	Ccr7	Chemokine (C–C motif) receptor 7			9.12			6.37			6.67				5.54		4.75	50.68
NM_007720	Ccr8	Chemokine (C–C motif) receptor 8		3.31										2.55	4.78	2.14		8.09
NM_009913	Ccr9	Chemokine (C–C motif) receptor 9	2.8		34.89	4.75	13.74	2.75		2.82	18.37				24.02		11.84	−2.65
NM_007768	Crp	C-reactive protein, pentraxin-related									2.72					4.58		−185.25
NM_009142	Cx3cl1	Chemokine (C–X3–C motif) ligand 1	8.38	6.39	9.74	4.8	12.06	9.38	15.3	3.49	6.86	3.37	−2.06	3.42	9.26	1.86	18.97	1.93
NM_008176	Cxcl1	Chemokine (C–X–C motif) ligand 1	−4.95		−7.57		−57.17		−5.78	5.85	−21.6		−135.12				−30.9	
NM_021274	Cxcl10	Chemokine (C–X–C motif) ligand 10	−37.21	−9.95			−31.03	−13.53			−3.81		−29.17	1.94	−5.8		−37.65	−20.11
NM_019494	Cxcl11	Chemokine (C–X–C motif) ligand 11	−4.42	−4.88				−10.46					−6.58		−3.63		−7.75	−12.97
NM_021704	Cxcl12	Chemokine (C–X–C motif) ligand 12		7.91		3.23	13.24	9.93	4.19	2.34					9.45		6.95	
NM_018866	Cxcl13	Chemokine (C–X–C motif) ligand 13		8.97		4.89		4.82			−2.37					2.26		
NM_011339	Cxcl15	Chemokine (C–X–C motif) ligand 15	−4.04	−6.3	5.28			−4.94	9.52								−4.96	728.33
NM_019932	Cxcl4	Chemokine (C–X–C motif) ligand 4			7.81						8.49	2.14				1.51		
NM_009141	Cxcl5	Chemokine (C–X–C motif) ligand 5	−24.59	3.27	−15.56	2.42	−48.07		−7.59	7.24	−11.8		−72.32		−7.65		−55.14	−8.39
NM_008599	Cxcl9	Chemokine (C–X–C motif) ligand 9		2.9									−2.66		4.28			−5.78
NM_009910	Cxcr3	Chemokine (C–X–C motif) receptor 3	7.86	4.26	6.45	4.03		7.31	16.83		9.49				10.83		10.29	−11.38
XM_894898	Ccr10	Chemokine (C–C motif) receptor 10		2.92		2.48		2.96		2.74	3.65				6.47	1.82		−19.14
NM_008337	Ifng	Interferon gamma						2.36					−3.08		3.75			−19.82
NM_010548	Il10	Interleukin 10		11.47				6.07					−2.91	4.06	13.38	2.95	3.49	−2.61
NM_008348	Il10ra	Interleukin 10 receptor, alpha	−5.66		4.72	3.18		2.19	6.01	2.68								
NM_008349	Il10rb	Interleukin 10 receptor, beta	2.27	3.47	2.6	2.18	4.26	3.03	3.78			2.52			3.19		4.02	37.59

Please cite this article in press as: J.D. Miller, et al., Inflammation-associated gene transcription and expression in mouse lungs induced by low molecular weight compounds from fungi from the built environment, Chem. Biol. Interact. (2009), doi:10.1016/j.cbi.2009.09.023

NM_008350	Il11	Interleukin 11			3.51					2.43				1.96	17.12	1.71	7.68	−61.08
NM_008355	Il13	Interleukin 13		1.09		9.44				6.23				4.29	3.88		4.6	−15.84
NM_133990	Il13ra1	Interleukin 13 receptor, alpha 1		1.47		2.07							−1.8					5.25
NM_008357	Il15	Interleukin 15	3.32	18.83			16.41	27.81	3.58	2.19					11.37		7.66	−1.72
NM_010551	Il16	Interleukin 16		2.07	3.16	3.51	2.89	3.54	12.39	1.78	7.65				4.07			
NM_019508	Il17b	Interleukin 17B											−4.09		2.43	2.64		−41.68
NM_008360	Il18	Interleukin 18	4.53	2.64	3.61		6.23	5.08	−2.64						6.4			2.62
NM_010554	Il1a	Interleukin 1 alpha									−3.25		−12.32					−2.22
NM_008361	Il1b	Interleukin 1 beta		3.18				2.63					−5.55					11.67
NM_019450	Il1f6	Interleukin 1 family, member 6									4.51			2.03	4.5	9.27	4.15	−21.3
XM_130058	Il1f8	Interleukin 1 family, member 8											−5.25					−224.07
NM_008362	Il1r1	Interleukin 1 receptor, type I	3.31		23.74		12.45		33.22		19.37				16.78		17.81	4.57
NM_010555	Il1r2	Interleukin 1 receptor, type II		7.03						2.82			−8.75					4.08
NM_021380	Il20	Interleukin 20																−503.68
NM_008368	Il2rb	Interleukin 2 receptor, beta chain			8.45	3.96	4.03		12.87		11.03	2.5			6.71			−8.42
NM_013563	Il2rg	Interleukin 2 receptor, gamma chain			8.22	3.41				2.51	5.81	2.18		2.4	3.12			745.68
NM_010556	Il3	Interleukin 3							3.12					−2.24	2.51			−1091.14
NM_021283	Il4	Interleukin 4						2.6									5.99	2.36
NM_008370	Il5ra	Interleukin 5 receptor, alpha	2.41	22.77				92.04		3.01		2.71		2.57	27.51		13.82	−11.43
NM_010559	Il6ra	Interleukin 6 receptor, alpha			4.09	2.85	2.19	2.44		2.24	5.73	2.31		2.01				7.72
NM_010560	Il6st	Interleukin 6 signal transducer	−9.04	−2.38	2.74		−4.25	−2.16	4.36	1.81	3.56	2.9		2.07	−5.13		−5.14	4.27
NM_009909	Il8rb	Interleukin 8 receptor, beta	−3.77			2.77	−2.12	2.43		2.35			−2.61	2.91			−3.79	41.58
NM_008401	Itgam	Integrin alpha M		9.97			4.03	10.52		3.28	3.69				7.31		3.54	334.04
NM_008404	Itgb2	Integrin beta 2	2.33								2.48							3.77
NM_010735	Lta	Lymphotoxin A					4.06			2.97					6.28			−57
NM_008518	Ltb	Lymphotoxin B		4.22	9.48	3.06	5.19	3.42	12.56	3.23	3.71	2.08		2.6				−3.32
NM_010798	Mif	Macrophage migration inhibitory factor	6.59	3.81	4.81		7.68	4.36	8.09						5.82		5.77	
NM_007926	Scye1	Small inducible cytokine sub-family E, member 1	4.87	2.5	4.48		4.26		3.8		4.29		1.6		4.19		3.48	1834.96
NM_009263	Spp1	Secreted phosphoprotein 1	3.87				2.66	4.16	2.12		3.33				4.18		3.76	7890.59
NM_011577	Tgfb1	Transforming growth factor, beta 1			3.72	2.98						2.48		2.2				8.71
NM_013693	Tnf	Tumor necrosis factor	−3.21		−3.05	2.35	−2.69		14.99		−2.41		16.17		5.44			
NM_011609	Tnfrsf1a	Tumor necrosis factor receptor superfamily, member 1a	5.4	5.88	4.03		6.14	5.99	6.21		5.35	2.33		2.26	5.57		5.86	615.49
NM_011610	Tnfrsf1b	Tumor necrosis factor receptor superfamily, member 1b				3.17				1.83			−3.95	1.88			−2.17	
NM_011616	Cd40lg	CD40 ligand	4.19	3.37	17.13		8.91	2.57	20.53		11.64	2.96			8.63		3.64	2.91
NM_023764	Tollip	Toll interacting protein										1.81						16.25
NM_011798	Xcr1	Chemokine (C motif) receptor 1										1.62			10.1		2.3	−44.32

Please cite this article in press as: J.D. Miller, et al., Inflammation-associated gene transcription and expression in mouse lungs induced by low molecular weight compounds from fungi from the built environment, Chem. Biol. Interact. (2009), doi:10.1016/j.cbi.2009.09.023

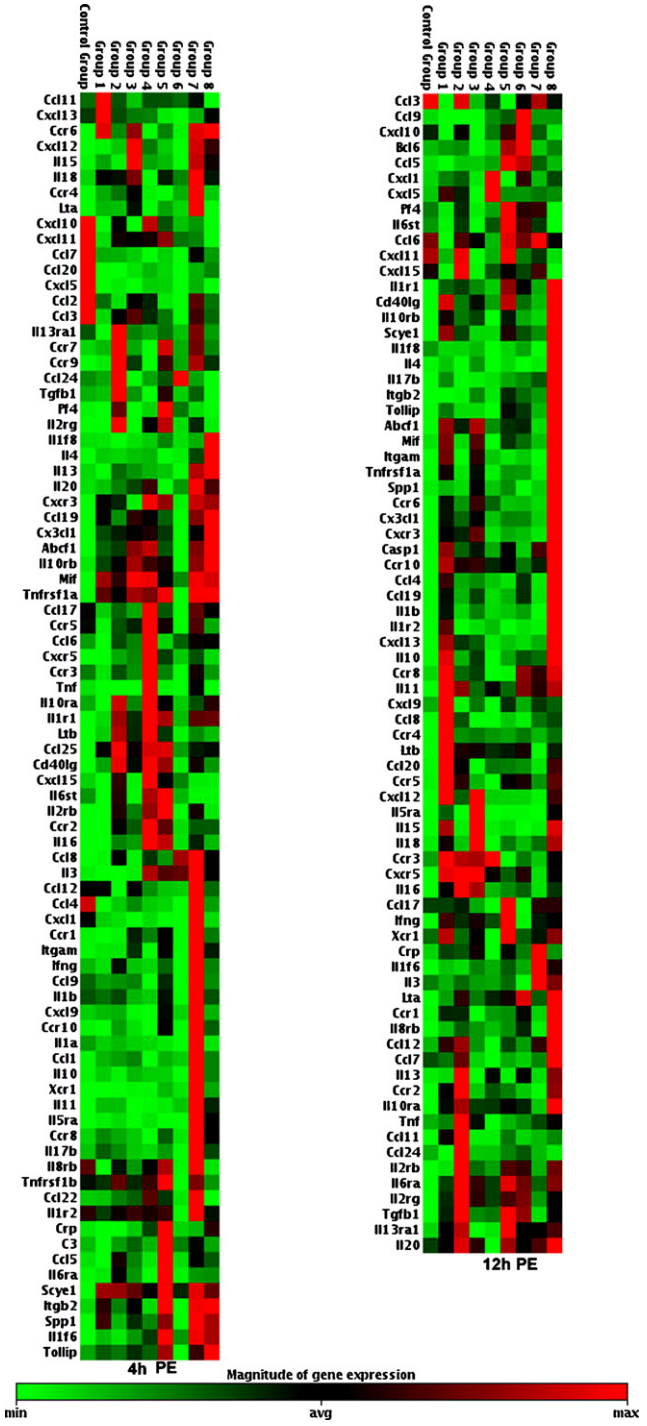

Fig. 3. Inflammation-associated gene expression heat maps showing significant ($p \leq 0.05$; $\geq$1.5-fold or ≥ -1.5-fold change) transcription patterns in mouse lungs intratracheally instilled with 4×10^{-5} moles/kg/lung wt at 4 h (a) and 12 h PE (b). Red and green cells signify genes that were either up- or down-regulated, respectively, after treatment compared to controls. The scale represents fold changes (red, up-regulated; green, down-regulated; black, average change). Control group = control animals; group 1 = atranone treatment; group 2 = treatment; group 3 = cladosporin treatment; group 4 = mycophenolic acid treatment; group 5 = neoechinulin A treatment; group 6 = neoechinulin B treatment; group 7 = sterigmatocystin treatment; group 8 = TMC-120A treatment. (For interpretation of the references to color in this figure legend, the reader is referred to the web version of the article.)

done by Ward's squared Euclidean distance method with SYSTAT v.12 software (San Jose, CA). Clusters were evaluated for significance using root mean square standard deviation and Calinski and Harabasz's pseudo-*F* analyses. At 12 h PE, three secure patterns of gene response (i.e. clusters) were obtained (1) brevianamide, mycophenolic acid and neoechinulin B, (2) neoechinulin A and sterigmatocystin, and (3) cladosporin, atranone C and TMC-120. A similar pattern was observed 4 h PE but the statistical significance was marginal.

3.4. Immunohistochemistry

MIP-2 and *Tnf-α* expression: Mouse skin positive control showed positive staining while control sections were unstained for both anti-*MIP-2* and anti-*Tnf-α* antibodies (data not shown). Carrier control stained lung tissues showed little or no evidence of positive staining. At both 4 h and 12 h PE bronchiolar epithelium apices of carrier controls (Fig. 4a) were lightly stained while alveolar walls were unstained (Fig. 4b) using both anti-*MIP-2* and anti-*Tnf-α* antibodies. At 4 h PE only light positive staining for *MIP-2* and *Tnf-α* was observed in lungs of treatment animals exposed to toxins (Fig. 4c). However, at 12 h PE, atranone C, brevianamide (Fig. 4d), cladosporin (Fig. 4e), mycophenolic acid, neoechinulin B, and TMC-120 instilled lungs revealed conspicuous anti-*MIP-2* antibody staining, while brevianamide, mycophenolic acid (Fig. 4f), neoechinulin B, and sterigmatocystin instilled lungs showed positive staining for anti-*Tnf-α* antibody. Positive staining with both antibody probes was generally in medial to apical regions of bronchiolar epithelium, and delineated by the unstained supporting basement membrane (Fig. 4c–e). Alveolar walls also showed patchy positive staining (Fig. 4f), which was usually associated with the cytoplasm of some but not all alveolar macrophages and alveolar type II cells (Fig. 5a and b) in toxin-instilled lungs probed using both anti-*MIP-2* and anti-*Tnf-α* antibody.

4. Discussion

The predominant taxa recovered from damp building materials are *Aspergillus*, *Eurotium*, *Penicillium* subgenus *Penicillium* species, and less commonly *Stachybotrys* species. All of the former species can produce low molecular weight toxins [40] although for most, little is known about their toxicities. A number of preliminary studies have been done for mycotoxins found in grain dusts on lung biology *in vivo* [18] and in primary alveolar cultures [23,41]. Few metabolites from fungi found indoors have been tested for biologically-relevant endpoints (i.e. not cytotoxicity) in lung cells lines or primary cultures of alveolar macrophages hence little is known about how they affect on lung biology *in vivo*.

There are only a few previous studies that address the issue of the inflammatory potential of pure toxins from fungi common on moist buildings using *in vivo* animal models. Most recently, Rand et al. [8,9] have shown that some pure metabolites of *Penicillium* species (brevianamide C, mycophenolic acid and roquefortine C) and *S. chartarum* toxin (atranones A and C) exposures result in a variety of inflammatory responses in intratracheally instilled 3-week-old CFW mice. These studies revealed that exposures resulted in increased concentrations of leukocytes (alveolar macrophages and neutrophils), pro-inflammatory cytokines and other hallmarks of pulmonary inflammation and damage in bronchioalveolar lavage fluid (BALF) in time-, dose- and toxin-dependent ways.

The results of the present study using histological, histochemical, immunohistochemical and gene array techniques further support the position that exposure to low doses of low molecular weight fungal compounds potentiates inflammatory lung responses. It is unclear whether these results are a consequence of

Please cite this article in press as: J.D. Miller, et al., Inflammation-associated gene transcription and expression in mouse lungs induced by low molecular weight compounds from fungi from the built environment, Chem. Biol. Interact. (2009), doi:10.1016/j.cbi.2009.09.023

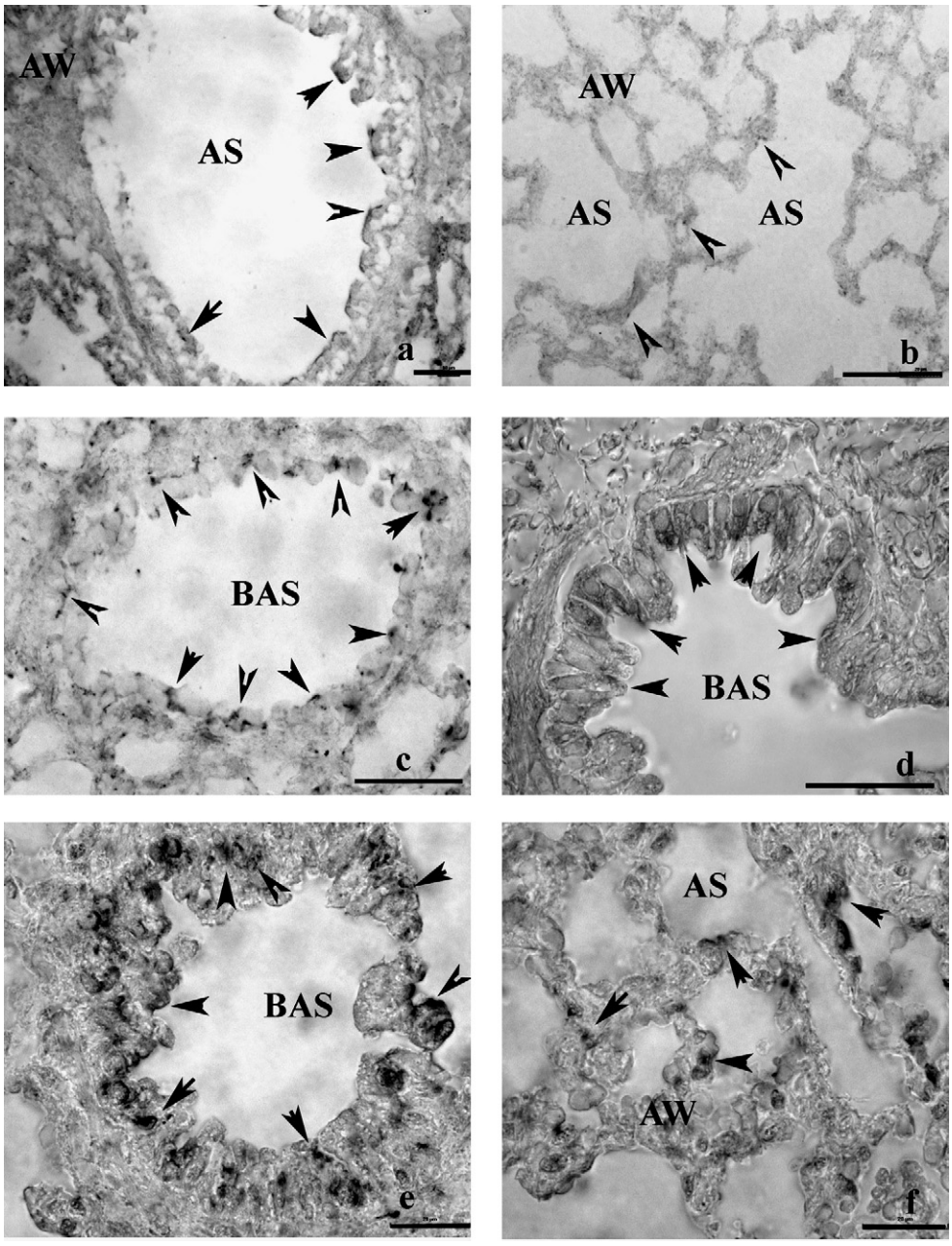

Fig. 4. Carrier control lungs at 12 h PE (a and b) showing modest apical staining of bronchiolar epithelium with anti-*MIP-2* antibody (a) (arrows) and apparent absence of stain on alveolar walls (arrows) (b). 4 h PE cladosporin exposed lung showing light apical bronchiolar epithelium staining with anti-*MIP-2* antibody (c) (arrows); 12 h PE brevianimide (d) and cladosporin (e) exposed lung showing conspicuous apical and medial bronchiolar epithelium staining with anti-*MIP-2* antibody (arrows); 12 h PE mycophenolic acid exposed lung showing positively stained alveolar walls with anti-*TNF-α* antibody (f) (arrows). AW = alveolar walls; AS = alveolar space; BAS = bronchiolar space. Bar scales = 20 μm. All treatment lungs were instilled with 4×10^{-5} mole toxin/kg/lung wt.

100% of the toxin impacting on the lung due to lack of absorption within 12 h PE because the toxicokinetics of each toxin is unknown. Further studies addressing this issue are needed.

For comparison, conidia and conidial fragments of *A. fumigatus*, which accumulates in settled dust indoors and under some circumstances will grow on building materials, accumulate fumitremorgens A, B and C, verruculogen, tryptacidin, and tryptoquivalene [42,43]. The sum conidial concentrations of the tremorgens fumitremorgens B and C and verruculogen were in the range ~1–14 $\mu g\, g^{-1}$ or $\sim 10^{-5}$ moles, depending on strain [43]. Conidia of *S. chartarum* were found to contain 10–15 $\mu g\, g^{-1}$ satratoxin G and trichoverrols A and B, or $\sim 10^{-5}$ moles [44]. These strains can produce other compounds in mycelia and their presence in condia as not been measured. Similar amounts of toxins of toxin have been reported in conidia and conidial fragments of *F. graminearum* and *F. sporotrichiodes*, and higher amounts ($\sim 10^{-4}$ moles) are reported from *A. flavus* and *A. parasiticus* [45].

Our histological observations revealed that toxin exposures resulted in a number of moderate anatomical lung changes including to bronchiolar epithelium profiles, and in the accumulation of leukocytes and amorphous and/or cellular debris in bronchiolar and alveolar spaces of all treatment animals at 12 h but not at 4 h PE. These results combined with histochemistry, which revealed accumulated muco-substances, especially in bronchiolar spaces and on apical bronchiolar epithelial surfaces at 12 h but not at 4 h PE suggests that responses are time-dependent and supports results of our previous studies showing significant time-dependent lung responses, including with some of the toxins used herein, at

Please cite this article in press as: J.D. Miller, et al., Inflammation-associated gene transcription and expression in mouse lungs induced by low molecular weight compounds from fungi from the built environment, Chem. Biol. Interact. (2009), doi:10.1016/j.cbi.2009.09.023

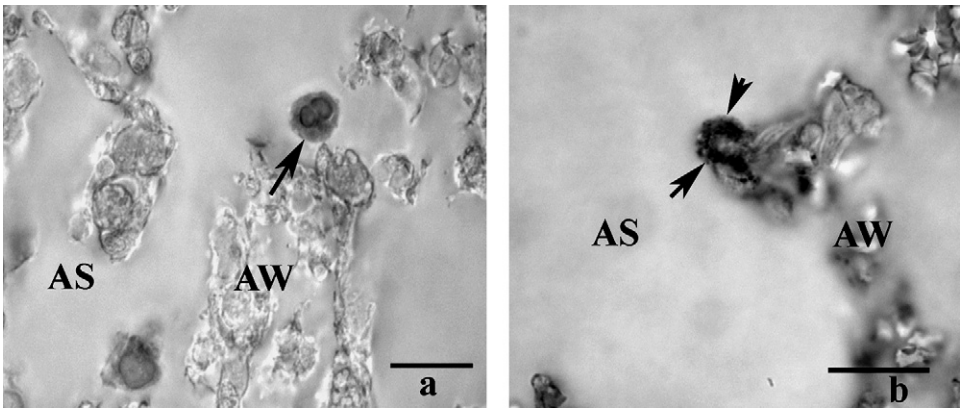

Fig. 5. Alveolar macrophage (arrow) in 12 h PE neoechinulin B instilled lung showing positive staining with anti-*MIP-2* antibody (a); alveolar type II cell in 12 h PE sterigmatocystin instilled lung showing positive stained using anti-*TNF-α* antibody (b). AW = alveolar walls; AS = alveolar space. Bar scales = 15 μm. All treatment lungs were instilled with 4×10^{-5} mole toxin/kg/lung wt.

6–48 h but not at 3 h PE [8,9]. The observation that the effects in all treatment animals were most apparent as changes associated with bronchiolar epithelium and leukocytes indicates that these cell changes may be a central event in the lung response to fungal toxin exposures. Moreover, that immunohistochemistry (IHC) showed localization of *MIP-2* and *Tnf-α* staining in respiratory bronchiolar epithelia, and in some but not all alveolar macrophages and alveolar type II cells compared to alveolar wall epithelia was interesting as these lining cells are located at one of the lung hot spots associated with sub-micron particle deposition in the lung [46]. This further confirms the important immunomodulatory role that these cells have in the response to low molecular weight fungal compounds [1].

Results of the array experiments revealed that compared to controls, all eight toxins from fungi associated with damp building materials induced pro-inflammatory responses manifest as significantly (generally up-regulated) transcribed inflammation-associated gene mRNAs in the lungs of intratracheally exposed mice. The significant transcription of the 10 genes in all treatment groups at either 4 and/or 12 h PE, as well as 16 genes in all but one treatment group was interesting. This result suggests that these genes may serve central roles in the orchestration of toxin-induced pro-inflammatory lung responses. The majority of these significantly modulated genes were ones associated with acute pulmonary inflammation (e.g. *Ccl19*, *Ccl20*, *Cxcl1*, *Cxcl5*, *Ltb*, *Scye1*, *Tnf-α*, *Cd40lg*), or their receptors (e.g. *Bir1*, *Ccr6*, *Ccr9*, *Ccr10*, *Cxcr3*, *Ilr1*, *Il10rb*, *Il2rb*, *Il6ra*, *Il6st*, *Tnfrsf1a*), especially in mediating acute inflammatory recruitment response of T-cells (*Ccl19*, *Ccl20*, *Ltb*, *Scye1*), alveolar macrophages (*Ccl25*, *TNF-α*), neutrophils (*Cxcl5*), and alveolar wall epithelium (*Cxcl5*, *Tnf-α*), amongst others [47–60]. *Cd40lg*, transcribed in all except neoechinulin B treated animals is a key signalling conduit to activate non-haematopoietic cells such as fibroblasts, and endothelial cells and to produce pro-inflammatory mediators [61]. Expression of transcriptionally regulated *Tnf-α* obtained using arrays, and *MIP-2* which has been shown to be expressed in the other animal exposure models [8,9], was confirmed at the protein level using IHC. The above-listed receptors, which were generally up-regulated in all treatment animals, are considered vitally important in neutrophil trafficking and amplification of inflammatory processes [64], pulmonary fibrosis [65] and the modulation of other cellular activities [62,63,66–69]. Significant transcription of these receptor and inflammation-associated gene mRNAs by the toxin treatments provides a mechanistic basis for the dose-dependent leukocyte responses in treatment rodent BALF observed in our earlier studies [8,9], and their apparent recruitment in respiratory tract tissues observed in this study.

The significant up-regulation of the *Abcf1* mRNA transcript in all treatment animals was also interesting. *Abcf1* is a sub-family member of genes associated with transporter/channel functions [61]. In lungs, activation of this gene is responsible for lamellar body formation, pulmonary surfactant secretion and considered to have a critical role in the metabolism of pulmonary phosphatidylglycerol (PG) [69]. Up-regulation of this gene may form a partial basis for the increased muco-substance production and accumulation in respiratory tract spaces and bronchiolar epithelium observed in the toxin treated animals, and account for increased phlegm production reported in some mold-exposed individuals [70]. This should be explored in further animal studies.

An important result of the study was the observation that mice exposed to toxins showed different gene transcription profiles. Amongst the most noticeable responses were those associated with sterigmatocystin and TMC-120 exposures at 12 h PE. Whereas sterigmatocystin exposures resulted in the modulation of relatively few genes (13/83), those of TMC-120 resulted in significant transcriptional changes in 68/83 genes. At present it is unclear why such different responses should result from toxin exposures. However, there are likely many factors that can affect toxin-induced lung inflammation mechanism of action and potency [see 8,9] as well as in toxicokinetics of inflammatory mediator release, toxin targeting, and different toxin clearance rates. Variations in any these factors would affect the dynamics and outcome of lung inflammation at the whole animal level. Despite the variations in toxin effects on lung inflammation outcome, cluster analysis revealed that they formed three distinct patterns of gene transcription which linked the response of the toxins at the same dose in particular groups. The clustering of brevianamide and neoechinulin B with mycophenolic acid is instructive because the latter is highly immunologically active based on an abundance of clinical and experimental data whereas the toxicities of the former have been unexplored. Similarly, the clustering of cladosporin and atranone C with TMC-120A links the former compounds previously suggested as not toxic with a compound which is again known highly immunologically active in humans. The clustering of the gene transcription patterns of neoechinulin A and sterigmatocystin links these compounds to biological effects in the related fungal toxin aflatoxin in humans and as well as to sterigmatocystin in *in vivo* and *in vitro* assays. This makes it difficult to rule out that exposure to very small amounts of fungal products from producer species as important in the health effects observed in exposed populations.

Based on what is known, toxin concentrations in spore and spore fragments of fungi that grow on damp building materials are in the order of $\sim 10^{-5}$ moles. Because there are 5-day air measurement data for β-glucan [71,72], as well as some concurrent PM2.5

Please cite this article in press as: J.D. Miller, et al., Inflammation-associated gene transcription and expression in mouse lungs induced by low molecular weight compounds from fungi from the built environment, Chem. Biol. Interact. (2009), doi:10.1016/j.cbi.2009.09.023

data [72], it is possible to make an exposure estimate. Brown et al. [73] provided lung PM2.5 dosimetry for resting and moderate nasal breathing and for moderate oral breathing, i.e. all particulate matters $\leq$2.5 μm in size, based on [71,74] comprise 70–90% of the total airborne β-glucan. On a 24-h basis, lung exposure to toxins in conidia and conidia fragments <2.5 μm for resting and moderate nasal breathing, and moderate oral breathing, would be 10^{-7}–10^{-8} moles, focused on a number of hot spots [46]. Prolonged exposure would represent an integration of cell response at least for a few days or 7–10 days, if the toxins acted like aflatoxin [18].

In summary, time- and toxin-dependent transcription and expression of inflammation-associated genes and inflammatory responses were observed in mouse lungs intratracheally exposed to eight different fungal toxins with the addition of 4–10^{-5} moles toxin/kg lung wt. These observations provide a biological basis for some of the inflammatory health effects reported from humans in damp building environments [2,70].

Conflict of interest

There are no conflicts of interest.

Acknowledgements

We thank C. Leggiadro, J. Monholland and C. Murphy, NRC Institute of Marine Biosciences, Halifax, Nova Scotia for assistance and excellent technical support. We also thank Dr. J. Pestka, Food Science and Human Nutrition, Michigan State University for his advice and critical reading of the manuscript and Dr. G. Sun (SMU) for use of the RT-PCR instrument. This work was supported by NSERC operating grants to T.G.R. and an NSERC IRC to J.D.M.

References

[1] T.G. Rand, M. Sun, A. Gilyan, J. Downey, J.D. Miller, Dectin-1 and inflammation-associated gene transcription and expression in mouse lungs by a toxic (1,3)-β-D glucan, Arch. Toxicol., in press.
[2] Health Canada, Fungal Contamination in Public Buildings: Health Effects and Investigation Methods, Health Canada, Ottawa, Ontario, 2004, ISBN 0-662r-r37432-0.
[3] J.D. Miller, Fungi as contaminants of indoor air, in: Proceedings 5th International Conference on Indoor Air Quality and Climate, vol. 5, Toronto, 1990, pp. 51–64.
[4] J.D. Miller, Fungi as contaminants of indoor air, Atmos. Environ. 26A (1992) 2163–2172.
[5] P.G. Holt, Inflammation in organic dust-induced lung disease: new approaches for research into underlying mechanisms, Am. J. Ind. Med. 17 (1990) 47–54.
[6] J. Flemming, B. Hudson, T.G. Rand, Comparison of inflammatory and cytotoxic lung responses in mice after intratracheal exposure to spores of two different *Stachybotrys chartarum* isolates, Toxicol. Sci. 78 (2004) 267–275.
[7] J.D. Miller, T.G. Rand, H. McGregor, J. Solomon, C. Yang, Mold ecology: recovery of fungi from certain moldy building materials, in: B. Prezant, D. Weekes, J.D. Miller (Eds.), Recognition, Evaluation and Control of Indoor Mold, American Industrial Hygiene Association, Fairfax, VA, 2008, pp. 43–51.
[8] T.G. Rand, S. Giles, J. Flemming, J.D. Miller, E. Puniani, Inflammatory and cytotoxic responses in mouse lungs exposed to purified toxins from building isolated *Penicillium brevicompactum* Dierckx and *P. chrysogenum* Thom, Toxicol. Sci. 87 (2005) 213–222.
[9] T.G. Rand, J. Flemming, J.D. Miller, T. Womiloju, Inflammatory and cytotoxic responses in mouse lungs toward atranones A and C from *Stachybotrys chartarum*, J. Toxicol. Environ. Health A 69 (2006) 1239–1251.
[10] H.K. Abbas, B.B. Johnson, W.T. Shier, H. Tak, B.B. Jarvis, C.D. Boyette CD, Phytotoxicity and mammalian cytotoxicity of macrocyclic trichothecene mycotoxins from *Myrothecium verrucaria*, Phytochemistry 59 (2002) 309–313.
[11] H. Anke, Metabolic products of microorganisms. 184. On the mode of action of cladosporin, J. Antibiot. (Tokyo) 32 (1979) 952–958.
[12] E. Bloom, L.F. Grimsley, C. Pehrson, J. Lewis, L. Larsson, Molds and mycotoxins in dust from water-damaged homes in New Orleans after hurricane Katrina, Indoor Air 19 (2009) 153–158.
[13] J. Bünger, G. Westphal, A. Monnick, B. Hinnendahl, E. Hallier, M. Müller, Cytotoxicity of occupationally and environmentally relevant mycotoxins, Toxicology 202 (2004) 199–211.
[14] R. De la Campa, Isolation and characterization of secondary metabolites from Canadian indoor strains of *Penicillium brevicompactum* and *P. chrysogenum*, M.Sc. Thesis, Carleton University, Ottawa, 2005.
[15] A.J. Delucca, J.J. Dunn, L.S. Lee, A. Ceigler, Toxicity, mutagenicity and teratogenicity of brevianamide, viomellein and xanthomegnin: secondary metabolites of *Penicillium viridicatum*, J. Food Safety 4 (1982) 165–168.
[16] S. Engelhart, A. Loock, D. Skutlarek, H. Sagunski, A. Lommel, H. Färber, M. Exner, Occurrence of toxigenic *Aspergillus versicolor* isolates and sterigmatocystin in carpet dust from damp indoor environments, Appl. Environ. Microbiol. 68 (2002) 3886–3890.
[17] H. Fujimoto, T. Fujimaki, Immunomodulatory constituents from an ascomycete, *Microascus tardifaciens*, Chem. Pharm. Bull. (Tokyo) 47 (1999) 1426–1432.
[18] G.J. Jakab, R.R. Hmieleski, A. Zarba, D.R. Hemenway, J.D. Groopman, Respiratory aflatoxicosis: suppression of pulmonary and systemic host defenses in rats and mice, Toxicol. Appl. Pharmacol. 125 (1994) 198–205.
[19] J. Grove, M. Pople, The insecticidal activity of some fungal dihydroisocoumarins, Mycopathologia 76 (1981) 65–67.
[20] J. Kohno, M. Sakura, N. Kameda, M. Nishio, K. Kawano, N. Kishi, T. Okuda, S. Komatsubara, Production, isolation and biological properties of TMC-120A, B, C, novel inhibitors of eosinophil survival from *Aspergillus ustus* TC 1118, J. Antibiot. 52 (1999) 913–916.
[21] K. Kuniaki, A. Toshiaki, S. Yasushi, K. Shinji, S. Fumio, K. Kouji, K. Atsuo, K. Susumu, K. Kenji, W. Nobuo, A. Takao, Structure–activity relationships of neoechinulin A analogues with cytoprotection against peroxynitrite-induced PC12 cell death, J. Antibiot. 60 (2007) 614–621.
[22] K. Kuramochi, K. Ohnishi, S. Fujieda, M. Nakajima, Y. Saitoh, N. Watanabe, T. Takeuchi, A. Nakazaki, F. Sugawara, T. Arai, S. Kobayashi, Synthesis and biological activities of neoechinulin A derivatives: new aspects of structure–activity relationships for neoechinulin A, Chem. Pharm. Bull. (Tokyo) 56 (2008) 1738–1743.
[23] B.H. Liu, F.Y. Yu, M.H. Chan, Y.L. Yang, The effects of mycotoxins, fumonisin B1 and aflatoxin B1, on primary swine alveolar macrophages, Toxicol. Appl. Pharmacol. 180 (2002) 197–204.
[24] K.F. Nielsen, S. Gravesen, P.A. Nielsen, B. Andersen, U. Thrane, J.C. Frisvad, Production of mycotoxins on artificially and naturally infested building materials, Mycopathologia 145 (1999) 43–56.
[25] K.F. Nielsen, K. Huttunen, A. Hyvärinen, B. Andersen B, B.B. Jarvis, M.R. Hirvonen, Metabolite profiles of *Stachybotrys* isolates from water-damaged buildings and their induction of inflammatory mediators and cytotoxicity in macrophages, Mycopathologia 154 (2002) 201–205.
[26] K.F. Nielsen, G. Holm, L.P. Uttrupa, P.A. Nielsen, Mould growth on building materials under low water activities. Influence of humidity and temperature on fungal growth and secondary metabolism, Int. Biodet. Biodeg. 54 (2004) 325–336.
[27] O.J. D'Cruz, F.M. Uckun, Dawn of non-nucleoside inhibitor-based anti-HIV microbicides, J. Antimicrob. Chemother. 57 (2006) 411–423.
[28] A. Ogawa, C. Murakami, S. Kamisuk, I. Kuriyama, H. Yoshida, F. Sugawara, Y. Mizushin, Pseudodeflectusin, a novel isochroman derivative from *Aspergillus pseudodeflectus*, a parasite of the sea weed, *Sargassum fusiform*, as a selective human cancer cytotoxin, Bioorg. Med. Chem. Lett. 14 (2004) 3539–3543.
[29] R.R.M. Paterson, M.J.S. Simmonds, C. Kemmelmeier, W.M. Blaney, Effects of brevianamide A, its photolysis product brevianamide D, and ochratoxin A from two *Penicillium* strains on the insect pests *Spodoptera frugiperda* and *Heliothis virescens*, Mycol. Res. 94 (1990) 538–542.
[30] M. Podojil, P. Sedmera, J. Vokoun, V. Betina, H. Barathova, Z. Durackova, K. Horakova, P. Nemec, *Eurotium* (*Aspergillus*) *repens* metabolites and their biological activity, Folia Microbiol. 23 (1978) 438–443.
[31] T. Tuomi, K. Reijula, T. Johnsson, K.L. Hemminki, E.-L. Hintikka, O. Lindroos, S. Kalso, P. Koukila-Kähkölä, H. Mussalo-Rauhamaa, T. Haahtela, Mycotoxins in crude building materials from water-damaged buildings, Appl. Environ. Microbiol. 66 (2000) 1899–1904.
[32] M. Umeda, T. Yamashita, M. Saito, S. Skeita, C. Takahashi, K. Yoshihira, S. Natori, H. Kurata, S. Udagawa, Chemical and cytotoxicity survey on the metabolites of toxic fungi, Jpn. J. Exp. Med. 44 (1974) 83–96.
[33] S. Wang, X.-M. Li, F. Teuscher, D.-L. Li, A. Diesel, R. Ebe, P. Proksch, B.-G. Wang, Chaetopyranin, a benzaldehyde derivative, and other related metabolites from *Chaetomium globosum*, an endophytic fungus derived from the marine red alga *Polysiphonia urceolata*, J. Nat. Prod. 69 (2006) 1622–1625.
[34] B.J. Wilson, D.T.C. Yang, M. Harris, Production, isolation, and preliminary toxicity studies of brevianamide A from cultures of *Penicillium viridicatum*, Appl. Environ. Microbiol. 26 (1973) 633–635.
[35] J.A. Yalowitz, K. Pankiewicz, S.E. Patterson, H.N. Jayaram, Cytotoxicity and cellular differentiation activity of methylenebis (phosphonate) analogs of tiazofurin and mycophenolic acid adenine dinucleotide in human cancer cell lines, Cancer Lett. 199 (2003) 107–108.
[36] G.J. Slack, E. Puniani, J.C. Frisvad, R.A. Samson, J.D. Miller, Secondary metabolites from *Eurotium* species, *A. calidoustus* and *A. insuetus* common in Canadian homes with a review of their chemistry and biological activities, Mycol. Res. 113 (2009) 480–490.
[37] CCAC Guide to the Care and Use of Experimental Animals, vol. 1, Bradda Printing Services, Ottawa, Ontario, 1993.
[38] L.G. Luna, Manual of Histologic Staining Methods of the Armed Forces Institute of Pathology, McGraw-Hill, Inc., 1968.
[39] R.F. Phalen, Methods in Inhalation Toxicology, CRC Press, Boca Raton, FL, 1997, p. 156.
[40] R.A. Samson, J.C. Frisvad, *Penicillium* subgenus Penicillium; new taxonomic schemes, mycotoxins and other extralites, Stud. Mycol. 49 (2004) 1–257.

Please cite this article in press as: J.D. Miller, et al., Inflammation-associated gene transcription and expression in mouse lungs induced by low molecular weight compounds from fungi from the built environment, Chem. Biol. Interact. (2009), doi:10.1016/j.cbi.2009.09.023

[41] W.G. Sorenson, G.F. Gerberick, D.M. Lewis, V. Castranova, Toxicity of mycotoxins for the rat pulmonary macrophage in vitro, Environ. Health Perspect. 66 (1986) 45–53.
[42] C.J. Land, A. Rask-Andersen, H. Lundström, S. Werner, S. Bardage, Tremorgenic mycotoxins and gliotoxin in conidia of *Aspergillus fumigatus*, in: R. Samson, B. Flannigan, M.E. Flannigan, S. Graveson S (Eds.), Health Implications of Fungi in Indoor Environments, Elsevier, Amsterdam, 1994, pp. 307–315.
[43] G. Fischer, T. Müller, R. Schwalbe, R. Ostrowski, W. Dott, Exposure to airborne fungi, MVOC and mycotoxins in biowaste-handling facilities, Int. J. Hyg. Environ. Health 203 (2000) 97–104.
[44] W.G. Sorenson, D.G. Frazer, B.B. Jarvis, J. Simpson, V.A. Robinson, Trichothecene mycotoxins in aerosolized conidia of *Stachybotrys atra*, Appl. Environ. Microbiol. 53 (1987) 1370–1375.
[45] T.G. Rand, J.D. Miller, Toxins and inflammatory compounds, in: B. Flannigan, R. Samson, J.D. Miller (Eds.), Microorganisms in Home and Indoor Work Environments: Diversity, Health Impacts, Investigation and Control, second edition, CRC Press, Boca Raton, FL, in press.
[46] R.F. Phalen, M.J. Oldham, R.K. Wolff, The relevance of animal models for aerosol studies, J. Aerosol Med. Pulm. Drug Deliv. 21 (2008) 113–124.
[47] A. Didierlaurent, B. Brissoni, D. Velin, N. Aebi, A. Tardivel, E. Käslin, J.C. Sirard, G. Angelov, J. Tschopp, K. Burns, Tollip regulates pro-inflammatory responses to interleukin-1 and lipopolysaccharide, Mol. Cell. Biol. 26 (2006) 735–742.
[48] C. Doucette, J. Giron-Michel, G.W. Canonica, B. Azzarone, Human lung myofibroblasts as effectors of the inflammatory process: the common receptor λ chain is induced by Th2 cytokines, and CD40 ligand is induced by lipopolysaccharide, thrombin and TNF-α, Eur. J. Immunol. 32 (2002) 2437–2449.
[49] A. Elizur, T.L. Adair-Kirk, D.G. Kelley, G.L. Griffin, D.E. de Mello, R.M. Senior, Tumor necrosis factor-α from macrophages enhances LPS-induced Clara cell expression of keratinocyte-derived chemokine, Am. J. Respir. Cell Mol. Biol. 38 (2008) 8–15.
[50] B. Hernandez-Novoa, L. Bishop, C. Logun, P.J. Munson, E. Elnekave, Z.G. Rangel, J. Barb, R.L. Danner, J.A. Kovacs, Immune responses to *Pneumocystis murina* are robust in healthy mice but largely absent in CD40 ligand-deficient mice, J. Leukocyte Biol. 84 (2008) 420–430.
[51] F. Huaux, M. Gharaee-Kermani, T. Liu, V. Morel, B. McGarry, M. Ullenbruch, S.L. Kunkel, J. Wang, Z. Xing, S.H. Phan, Role of Eotaxin-1 (*CCL11*) and CC chemokine receptor 3 (*CCR3*) in bleomycin-induced lung injury and fibrosis, Am. J. Pathol. 167 (2005) 1485–1496.
[52] Y. Ishida, A. Kimura, T. Kondo, T. Hayashi, M. Ueno, N. Takakura, K. Matsushima, N. Mukaida, Essential roles of the CC chemokine ligand 3-CC chemokine receptor 5 axis in bleomycin-induced pulmonary fibrosis through regulation of macrophage and fibrocyte infiltration, Am. J. Pathol. 170 (2007) 843–854.
[53] S. Jeyaseelan, R. Manzer, S.K. Young, M. Yamamoto, S. Akira, R.J. Mason, G.S. Worthen, Induction of *CXCL5* during inflammation in the rodent lung involves activation of alveolar epithelium, Am. J. Respir. Cell Mol. Biol. 32 (2005) 531–539.
[54] J. Kaufman, P.J. Sime, R.P. Phipps, Expression of CD154 (CD40 ligand) by human lung fibroblasts: differential regulation by *IFN-λ* and *IL-13*, and implications for fibrosis, J. Immunol. 172 (2004) 1862–1871.
[55] S.G. Kelsen, M.O. Aksoy, Y. Yang, S. Shahabuddin, J. Litvin, F. Safadi, T.J. Rogers, The chemokine receptor *CXCR3* and its splice variant are expressed in human airway epithelial cells, Am. J. Physiol. Lung Cell. Mol. Physiol. 287 (2004) L584–L591.
[56] K. Murphy, P. Travers, M. Walport, Janeway's Immunobiology, Garland Science, Taylor & Francis, New York, 2008.
[57] Y. Ohkawara, X.F. Lei, M.R. Stampfli, J.S. Marshall, Z. Xing, M. Jordana, Cytokine and eosinophil responses in the lung, peripheral blood, and bone marrow compartments in a murine model of allergen-induced airways inflammation, Am. J. Respir. Cell Mol. Biol. 16 (2005) 510–520.
[58] J.E. Pease, I. Sabroe, The role of interleukin-8 and its receptors in inflammatory lung disease: implications for therapy, Am. J. Respir. Med. 1 (2002) 19–25.
[59] Y. Suzaki, K. Hamada, T. Nomi, T. Ito, M. Sho, Y. Kai, Y. Nakajima, H. Kimura, A small-molecule compound targeting *CCR5* and *CXCR3* prevents airway hyperresponsiveness and inflammation, Eur. Respir. J. 31 (2008) 783–789.
[60] N. Yamashita, H. Tashimo, Y. Matsuo, H. Ishida, K. Yoshiura, K. Sato, N. Yamashita, T. Kakiuchi, K. Ohta, Role of *CCL21* and *CCL19* in allergic inflammation in the ovalbumin-specific murine asthmatic model, J. Allergy Clin. Immunol. 117 (2006) 1040–1046.
[61] M. Richard, R. Droun, A.D. Beaulieu, ABC50, a novel human *ATP*-binding cassette protein found in tumor necrosis factor-α stimulated synoviocytes, Genomics 53 (1998) 137–145.
[62] T. Yoshimura, Chemokine receptors and neutrophil trafficking, in: J.K. Harrison, N.W. Lukacs (Eds.), The Chemokine Receptors, Human Press, NJ, 2007, pp. 71–86.
[63] G. Trujillo, C.M. Hogaboam, Chemokines and their receptors in fibrosis, in: J.K. Harrison, N.W. Lukacs (Eds.), The Chemokine Receptors, Human Press, NJ, 2007, pp. 295–317.
[64] J.J. Osterholzer, T. Ames, T. Polak, J. Sonstein, B.B. Moore, S.W. Chensue, G.B. Toews, J.L. Curtis, *CCR2* and *CCR6*, but not endothelial selectins, mediate the accumulation of immature dendritic cells within the lungs of mice in response to particulate antigen, J. Immunol. 175 (2005) 874–883.
[65] S. Uehara, A. Grinberg, J.M. Farber, P.E. Love, A role for CCR9 in T lymphocyte development and migration, J. Immunol. 168 (2002) 2811–2819.
[66] L.O. Cardell, R. Uddman, Y. Zhang, M. Adner, Interleukin-1beta up-regulates tumor necrosis factor receptors in the mouse airways, Pulm. Pharmacol. Ther. 21 (4) (2008) 675–681.
[67] M.I. Gómez, S.H. Sokol, A.B. Muir, G. Soong, J. Bastien, A.S. Prince AS, Bacterial induction of *TNF-alpha* converting enzyme expression and *IL-6* receptor alpha shedding regulates airway inflammatory signaling, J. Immunol. 175 (2005) 1930–1936.
[68] C. Pantano, V. Anathy, P. Ranjan, N.H. Heintz, Y.M. Janssen-Heininger, Nonphagocytic oxidase 1 causes death in lung epithelial cells via a *TNF-RI-JNK* signaling axis, Am. J. Respir. Cell Mol. Biol. 36 (2007) 473–479.
[69] M.L. Fitzgerald, R. Xavier, K.J. Haley, R. Welti, J.L. Goss, C.E. Brown, D.Z. Zhuang, S.A. Bell, N. Lu, M. McKee, B. Seed, M.W. Freeman, ABCA3 inactivation in mice causes respiratory failure, loss of pulmonary surfactant, and depletion of lung phosphatidylglycerol, J. Lipid Res. 48 (2007) 621–632.
[70] NAS, Damp Indoor Air Spaces and Health, National Academies Press, Washington, DC, 2004.
[71] M. Foto M, L.L.P. Vrijmoed, J.D. Miller, K. Ruest, M. Lawton, R.E. Dales, Comparison of airborne ergosterol, glucan and Air-O-Cell data in relation to physical assessments of mold damage and some other parameters, Indoor Air 15 (2005) 256–266.
[72] J.D Miller, R. Dugandzic, A.-M. Frescura, V. Salares, Indoor and outdoor-derived contaminants in urban and rural homes in Ottawa, Canada, J. Air Waste Manage. Assoc. 57 (2007) 297–302.
[73] J.S. Brown, W.E. Wilson, L.D. Grant, Dosimetric comparisons of particle deposition and retention in rats and humans, Inhal. Toxicol. 17 (2005) 355–385.
[74] V.R. Salares, C.A. Hinde, J.D. Miller, Analysis of settled dust in homes and fungal glucan in air particulate collected during HEPA vacuuming, Indoor Built Environ., in press.

Please cite this article in press as: J.D. Miller, et al., Inflammation-associated gene transcription and expression in mouse lungs induced by low molecular weight compounds from fungi from the built environment, Chem. Biol. Interact. (2009), doi:10.1016/j.cbi.2009.09.023